

# Bifurcation Analysis of Neuronal Bursters Models

B. Knowlton, W. McClure, N. Vu

REU Final Presentation  
August 3, 2017

- Introduction
- Stability
- Bifurcations
- The Hindmarsh-Rose Model
- Our Contributions

- Neurons are the fundamental unit of the brain.
- Rapid increases/decreases in electric potential allow for communication between neurons.
- Spiking and bursting are the big two.
- Models that can spike and burst are called neuronal burster models.

# Ion Dynamics — Ion Channels

- Tunnels within the cell membrane, which can be opened or closed
- Triggered by input signals, including the presence of ions and voltage
- Diffusive motion only

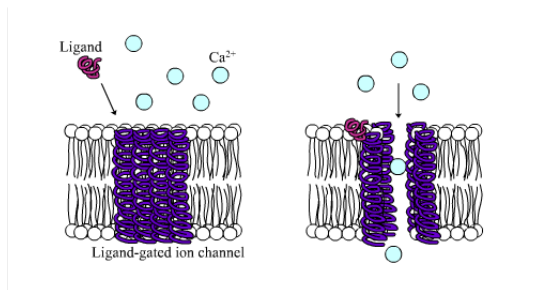
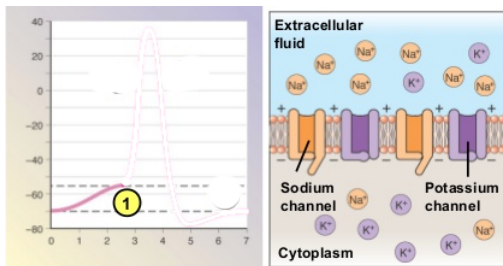


Figure: A ligand-gated calcium ion channel.

# Neuron Firing in General

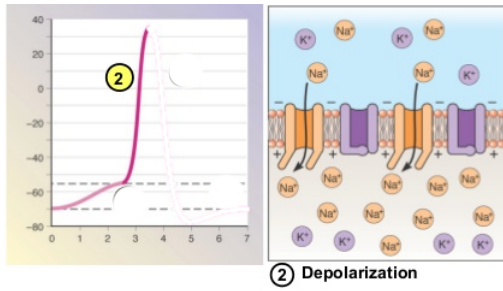
- This is not exactly the process we're modelling — more on that later
- *Resting potential*: the cell has a voltage of  $-70\text{mV}$ . More  $\text{K}^+$  inside, more  $\text{Na}^+$  outside.



① Resting state

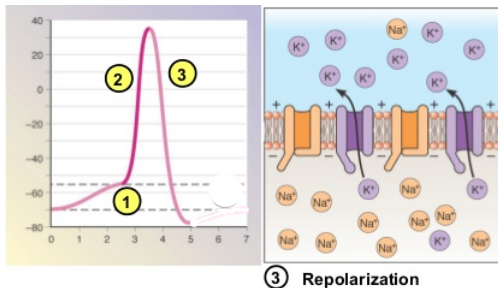
# Depolarization

- *Action potential* occurs when voltage reaches -55mV
- Voltage-gated  $\text{Na}^+$  channels open, increasing voltage
- Feedback loop



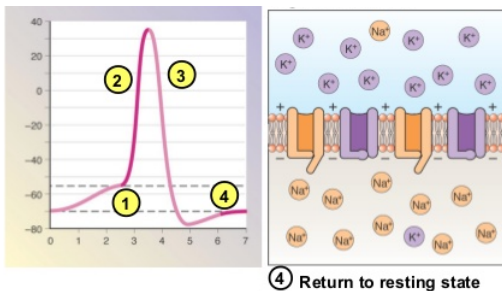
# Repolarization

- $\text{Na}^+$  channels close after a time
- $\text{K}^+$  channels are opened, letting voltage decrease
- Overshoot



# Getting Back to Resting Potential

- Various processes return the neuron to its initial state





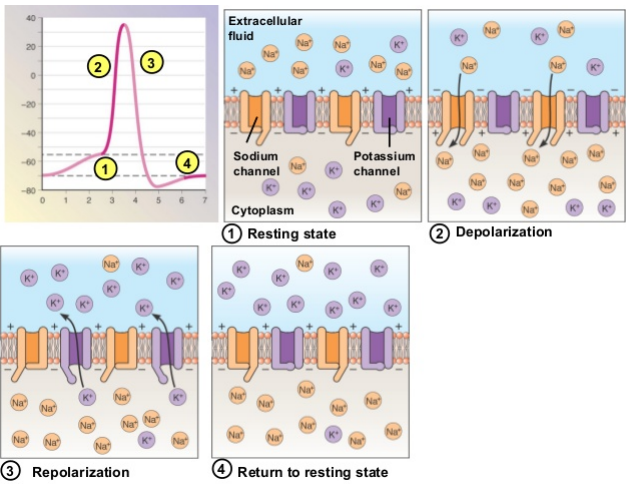


**Figure:** Visual representation of the flow of ions in the neuron cell during spiking behavior. [2]

- Nonlinear systems of the form

$$x(t)' = f(x(t)), \quad f : \mathbb{R}^n \rightarrow \mathbb{R}^n. \quad (1)$$

- Typically impossible to obtain explicit solutions
- We want to characterize qualitative behavior of solutions without getting the actual solutions

- A set  $S \subset \mathbb{R}^n$  is called invariant with respect to a dynamical system  $x' = f(x)$  if for any initial vector  $x(t_0) = x_0 \in S$ , the solution  $x(t)$  remains in  $S$  for all time  $t \geq t_0$ .
- Typical examples include equilibrium points and periodic orbits.

# Stability of Equilibrium Points

- An equilibrium point  $x_0 \in \mathbb{R}^n$  is stable if for all  $\epsilon > 0$ , there exists a  $\delta > 0$  such that

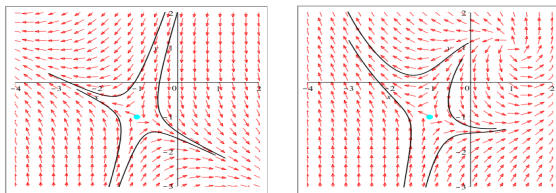
$$\|x(0) - x_0\| < \delta \implies \|x(t) - x_0\| < \epsilon \quad (2)$$

for all  $t > 0$ .

- Asymptotic stability:  $\lim_{t \rightarrow \infty} x(t) = x_0$ .
- Unstable points are not stable
- Analysis can be on local or global scales

# Local Stability

- A linearization of a system  $x' = f(x)$  at  $x_0$  is  $x' = Ax$  where  $A = Df(x_0)$
- The strategy is to locate equilibria and study their linearizations at those points. The linear system behavior informs us about neighborhoods in the nonlinear system.



- How do we know linearized models are reliable?

# Stable Manifold Theorem

## Theorem

Let  $E \subset \mathbb{R}^n$  be open containing the origin,  $f \in C^1(E)$ , and let  $\phi_t$  be the flow of  $x' = f(x)$ . Suppose the origin is a hyperbolic equilibrium point and that  $A = Df(0)$  has  $k$  eigenvalues with negative real part and the remaining  $n - k$  eigenvalues have positive real part. Then,

- (a) There exists a  $k$ -dimensional differentiable manifold  $S$  tangent to  $E^s$  (stable subspace of the linearization) at the origin, such that  $\phi_t(S) \subset S, \forall t \geq 0$  and  $\lim_{t \rightarrow \infty} \phi_t(x) = 0, \forall x \in S$ .
- (b) There exists an  $(n - k)$ -dimensional differentiable manifold  $U$  tangent to  $E^u$  (unstable subspace of the linearization) at the origin, such that  $\phi_t(U) \subset U, \forall t \leq 0$  and  $\lim_{t \rightarrow -\infty} \phi_t(x) = 0, \forall x \in U$ .

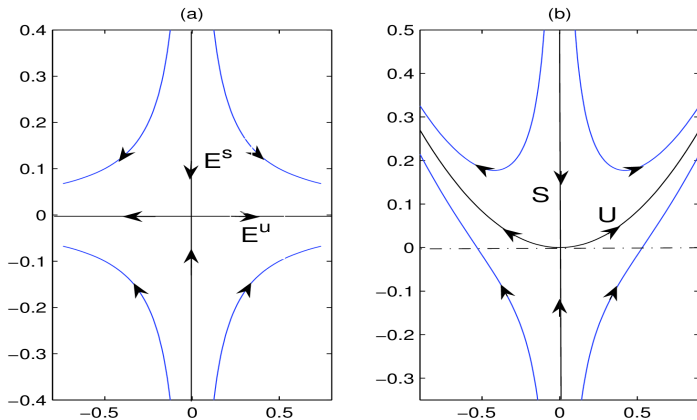
## Theorem

*Let  $x_0$  be a hyperbolic equilibrium of the nonlinear system (1). Then, in a neighborhood of  $x_0$ , the system (1) and its corresponding linearization*

$$\dot{x} = Ax, \quad (3)$$

*where  $A = Df(x_0)$ , are equivalent; that is, there is a homeomorphism  $h$  that maps trajectories in (1) near  $x_0$  onto trajectories in (3).*

# Linearization



These theorems also work together for  $n \geq 2$



- Global theory provides techniques to determine large regions in  $\mathbb{R}^n$  that may act as attracting or repelling basins.
- Global stability implies local stability, but the converse is not true in general.
- Lyapunov function analysis
  - Works on arbitrary equilibrium points — hyperbolic *and* nonhyperbolic

# Theorem to find Global Stability

## Theorem

Let  $E$  be an open subset of  $\mathbb{R}^n$  containing  $x_0$ . Suppose that  $f \in C^1(E)$  and that  $f(x_0) = 0$ . Suppose further that there exists a real valued function  $V \in C^1(E)$  satisfying  $V(x_0) = 0$  and  $V(x) > 0$  if  $x \neq x_0$ . Then

- (a) if  $V'(x) \leq 0$  for all  $x \in E$ ,  $x_0$  is stable;
- (b) if  $V'(x) < 0$  for all  $x \in E \sim \{x_0\}$ ,  $x_0$  is asymptotically stable;
- (c) if  $V'(x) > 0$  for all  $x \in E \sim \{x_0\}$ ,  $x_0$  is unstable.

- The function  $V$  satisfying these conditions is called a Lyapunov function.
- Constructing a Lyapunov function:
  - Matrix-theoretic method
  - Graph-theoretic method

## Theorem

(Shuai and Van Den Driessche's Theorem) Suppose that the following assumptions are satisfied:

- 1 There exists function  $D_i : U \rightarrow R$ ,  $G_{ij} : U \rightarrow R$  and constant  $a_{ij} \geq 0$  such that for every  $1 \leq i \leq n$ ,  
 $D'_i = D'_i|_{(3.6)} \leq \sum_{j=1}^n a_{ij} G_{ij}(z)$  for  $z \in U$ .
- 2 For  $A = [a_{ij}]$ , each directed cycle  $C$  of  $(G, A)$  has  
 $\sum_{(s,r) \in (C)} G_{rz}(z) \leq 0$  for  $z \in U$ , where  $(C)$  denotes the arc set of the directed cycle  $C$ .

Then, the function

$$D(z) = \sum_{i=1}^n c_i D_i(z) \quad (4)$$

with constant  $c_i \geq 0$  satisfies  $D' = D'|_{(3.6)} \leq 0$ ; that is,  $D$  is a Lyapunov function [5].

The next two theorems can be used to find  $c_i$ .

### Theorem

*If  $a_{ij} > 0$  and  $d^+(j) = 1$  for some  $i, j$  then*

$$c_i a_{ij} = \sum_{k=1}^n c_j a_{jk}$$

### Theorem

*If  $a_{ij} > 0$  and  $d^-(i) = 1$  for some  $i, j$  then*

$$c_i a_{ij} = \sum_{k=1}^n c_k a_{ki}$$

## Theorem

(LaSalle's Theorem) *Let  $\Omega \subset D \subset \mathbb{R}^n$  be a compact positively invariant set with respect to the system dynamics. Let  $V : D \rightarrow \mathbb{R}$  be a continuously differentiable function such that  $V'(x(t)) \leq 0$  in  $\Omega$ . Let  $E \subset \Omega$  be the set of all points in  $\Omega$  where  $V'(x) = 0$ . Let  $M \subset E$  be the largest invariant set in  $E$ . Then every solution starting in  $\Omega$  approaches  $M$  as  $t \rightarrow \infty$ , that is*

$$\lim_{t \rightarrow \infty} \left( \inf_{z \in M} \|x(t) - z\| \right) = 0 \quad (5)$$

*Notice that the inclusion of the sets in the LaSalle's theorem is:*

$$M \subset E \subset \Omega \subset D \subset \mathbb{R}^n$$

- In most applications, the vector field  $f$  depends on one or more parameters, that is, the dynamical systems take the form

$$x(t)' = f(x(t), \mu) \quad (6)$$

with  $\mu \in \mathbb{R}^p$  for some positive integer  $p$ .

- In general, solutions of (6) will vary as the parameters vary, but most importantly, there are special values of the parameters, say  $\mu = \mu_0$ , such that an arbitrarily small variation around  $\mu_0$  will cause drastic changes in the qualitative behavior of the solutions.

# Codimension-1 Bifurcations

- The codimension of a bifurcation is the minimum number of parameters necessary for the system (6) to experience a drastic change.
- These changes include:
  - The number of eq. points
  - Stability properties
  - Creation/destruction of special solutions
- The following bifurcations are common codimension-one bifurcations

- Consider the following system of equations:

$$\begin{aligned}x' &= \mu x - x^2 \\y' &= \mu x^2 - y\end{aligned}\tag{7}$$

with parameter  $\mu$ . The value of  $\mu$  alone can determine how solutions of this system behave, so there will be a codimension-1 bifurcation.



# Transcritical Bifurcation

- This type of bifurcation is characterized by an exchange of stability at bifurcation values (a stable equilibrium becomes unstable and an unstable one becomes stable).

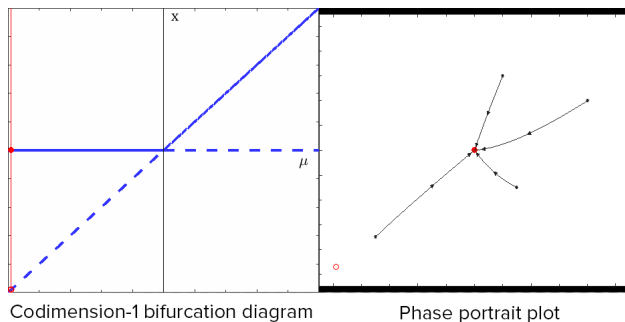
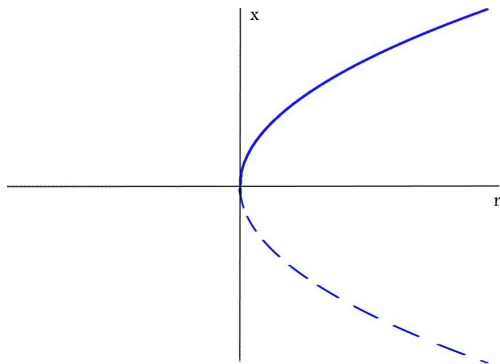


Figure: Animation showing a transcritical bifurcation in (7) with varying  $\mu$ .

# Saddle-node Bifurcation

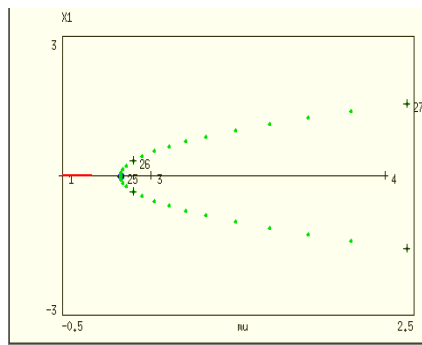
- In this type of bifurcations, equilibria coalesce in such a way that the number of equilibria can go from two to one to none: equilibria collide and annihilate one another.



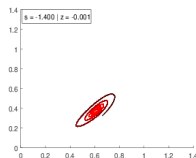
Saddle-Node bifurcation diagram.

# Hopf Bifurcation

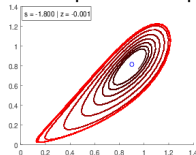
- This type of bifurcation is characterized by a stable (focus) equilibrium point losing stability, and one or more periodic solutions appearing in the system.



Bifurcation diagram



Before Hopf - stable spiral



After Hopf - unstable spiral,  
stable per. orbit

## Theorem

*Suppose that  $f(x_0, \mu_0) = 0$  and that the  $n \times n$  matrix  $A \equiv Df(x_0, \mu_0)$  has a simple eigenvalue of  $\lambda = 0$  with the eigenvector  $v$  and that  $A^T$  has an eigenvector  $w$  corresponding to the eigenvalue  $\lambda = 0$ . Further more, suppose that  $A$  has  $k$  eigenvalues with negative real part and  $(n-k-1)$  eigenvalues with positive real part. Then the following three sets of conditions correspond with different types of bifurcations:*

- *There is a saddle-node bifurcation if*

$$\begin{aligned}w^T f_\mu(x_0, \mu_0) &\neq 0, \\w^T [D^2 f(x_0, \mu_0)(v, v)] &\neq 0\end{aligned}$$

## Theorem

- *There is a transcritical bifurcation if*

$$w^T f_\mu(x_0, \mu_0) = 0$$

$$w^T [Df_\mu(x_0, \mu_0)v] \neq 0$$

$$w^T [D^2f(x_0, \mu_0)(v, v)] \neq 0$$

- *There is a pitchfork bifurcation if*

$$w^T f_\mu(x_0, \mu_0) = 0$$

$$w^T [Df_\mu(x_0, \mu_0)v] \neq 0$$

$$w^T [D^2f(x_0, \mu_0)(v, v)] = 0$$

$$w^T [D^3f(x_0, \mu_0)(v, v, v)] = 0$$

- This theorem is used later on to prove bifurcations in the system we are studying.

# The Hopf Bifurcation Theorem

## Theorem

*If  $\sigma \neq 0$ , then a Hopf bifurcation occurs at the origin of the planar analytic system (2) at the bifurcation value  $\mu = 0$ ; in particular, if  $\sigma < 0$ , then a unique stable limit cycle bifurcates from the origin of (2) as  $\mu$  increases from zero and if  $\sigma > 0$ , then a unique unstable limit cycle bifurcates from the origin of (2) as  $\mu$  decreases from zero. If  $\sigma < 0$ , the local phase portraits for (2) are topologically equivalent to those in the nonlinear system.*

$$\begin{aligned}x' &= \mu x - y + p(x, y) \\y' &= x + \mu y + q(x, y) \quad (2)\end{aligned}$$

# Higher-Codimension Bifurcations

- The behavior of solutions will depend on the changes of more than one control parameter.
- This can lead to a curve of bifurcation points.
- Keep in mind that detecting one single bifurcation point is complicated. Here we try to find continuous curves of bifurcation points that collide to form a codimension-2 bifurcation
- The following are some common codimension-2 bifurcations.

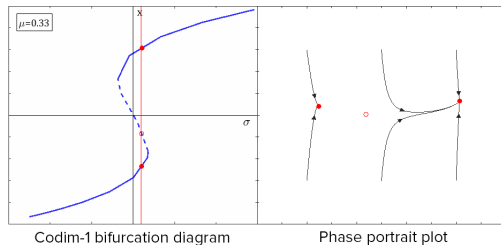
## Second Example

- Consider now the system

$$\begin{aligned}x' &= \sigma + \mu x - x^3 \\y' &= \mu x^3 - y\end{aligned}\tag{8}$$

with two parameters,  $\mu$  and  $\sigma$ .

- If we hold  $\mu=0.33$  constant, then there are two saddle-nodes in  $\sigma$  (codim-1):





# Cusp Bifurcation

- A codimension-2 saddle-node bifurcation happens when two curves of saddle-nodes bifurcations collide, so there are two saddle-node curves before the bifurcation (before the collision), and none after that. This is known as a cusp.

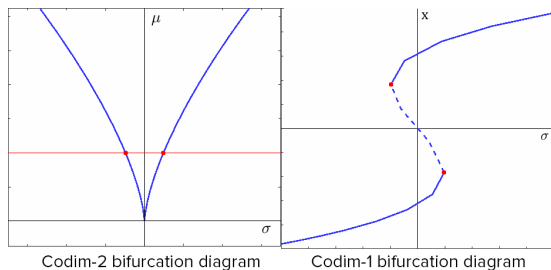


**Figure:** An animation displaying the changes in  $\sigma$  bifurcation diagrams as  $\mu$  varies.

# Bogdanov-Takens Bifurcation

- When a curve of saddle-node bifurcations collides with a curve of Hopf bifurcations (each point on this curve represents a codimension-1 Hopf bifurcation), then we get codimension-2 Bogdanov-Takens bifurcation

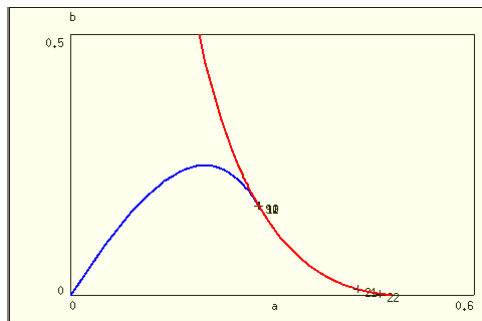


**Figure:** Example of Bogdanov-Takens bifurcation on XPPaut. The saddle-node bifurcation is in red and the Hopf bifurcation is in blue.

# Bautin or Generalized Hopf Bifurcation

- Suppose we have two distinct curves of (codimension-1) Hopf bifurcations, one generating stable periodic orbits (supercritical) and the other generating unstable orbits (subcritical).
- When two such curves collide, we have a so called Bautin (or Generalized Hopf) bifurcation.

# Bautin or Generalized Hopf Bifurcation

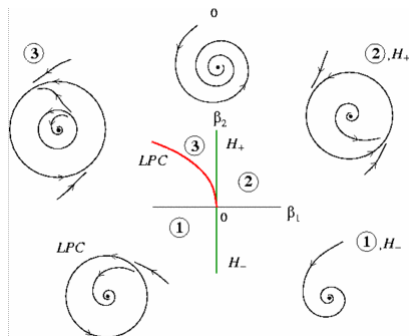
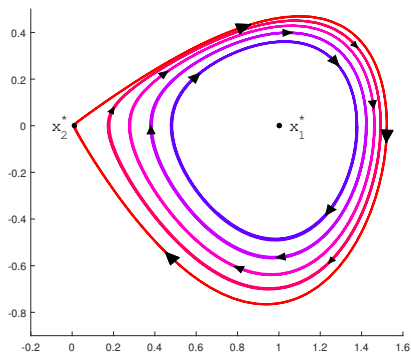


**Figure:** Generalized Hopf bifurcation diagram. The vertical axis corresponds to the Hopf bifurcation (supercritical at  $H_-$  and subcritical at  $H_+$ ); the curve LPC corresponds to the saddle-node bifurcation of periodic orbits. The phase portraits drawn in the margins indicate solution behavior in each region of parameter space [3].

- All previous examples were **local bifurcations** — collisions of *equilibrium points* (or curves of equilibrium points)
- **Global bifurcations** — collisions of *periodic orbits* with equilibrium points or each other

# Homoclinic Bifurcation



Periodic orbits with increasing period that eventually turns into a **homoclinic connection**.

# Homoclinic Bifurcation

In a Homoclinic bifurcation, the period of a periodic orbit (around some equilibrium point  $x_2^*$ ) grows so large that the periodic orbit itself collides with an equilibrium point  $x_1^*$ , generating a homoclinic connection, that is special solution of the system which connect  $x_1^*$  to itself, after wandering far away from it.

## Definition

Suppose  $x_0 \in \mathbb{R}^n$  is an equilibrium point of the system  $x' = f(x)$ . We say that a trajectory or a solution  $x(t)$  of this system is a homoclinic connection if

$$x(t) \longrightarrow x_0, \quad \text{as } t \longrightarrow \pm\infty$$



- Hodgkin-Huxley model: describes the biology very well, but is complicated

$$V'_m = -\frac{1}{C_m} (I_{Ca} + I_K + I_{K_{Ca}})$$

$$n' = \frac{n_{\infty}(V_m) - n}{\tau_n}$$

$$c' = -f_c (\alpha I_{Ca}(V_m) + k_{PMCA}c)$$

$$I_{Ca}(V_m) = g_{Ca} m_{\infty}^2(V_m)(V_m - V_{Ca})$$

$$I_K(V_m, n) = g_K n(V_m - V_K)$$

$$I_{K_{Ca}}(V_m, c) = g_{K_{Ca}} s_{\infty}(c)(V_m - V_K)$$

$$m_{\infty}(V_m) = \left( 1 + \exp\left(\frac{V_{mL} - V_m}{s_m}\right) \right)^{-1}$$

$$n_{\infty}(V_m) = \left( 1 + \exp\left(\frac{V_n - V_m}{s_n}\right) \right)^{-1}$$

$$s_{\infty}(c) = \frac{c^4}{c^4 + k_s^4}$$

- Three variables; fourteen parameters

- Fitzhugh-Nagumo Model: a reduction of the HH model.
- Much simpler, but cannot reproduce all the same behaviors

$$v' = v - \frac{v^3}{3} - w + I_{\text{ext}}$$
$$w' = \frac{1}{\tau} (v + a - bw)$$

- Two variables; four parameters

The Hindmarsh-Rose model has three variables and eight parameters. It's simpler than the HH model, but can also replicate all of its behaviors.

- $x(t)$ : Membrane potential (primary output variable)
- $y(t)$ : A measure of activity in voltage-gated potassium channel (**fast variable**)
- $z(t)$ : Cytosolic calcium (**slow variable**)

$$x' = -s(-ax^3 + x^2) - y - bz$$

$$y' = \phi(x^2 - y)$$

$$z' = \epsilon(sa_1x + b_1 - kz)$$

# HR Model: Slightly Different

- Instead of  $\text{Na}^+$ ,  $\text{Ca}^{2+}$  causes depolarization.
- $\text{Ca}^{2+}$  opens some  $\text{K}^+$  channels, so it plays a part in repolarization too.

# Physical Interpretations of Parameters

$s$  : A weight on depolarization dynamics for both  $x'$  and  $z'$ .

$a$  : How much the "high point" of depolarization influences  $x'$ .

$a_1$  : Calcium gate sensitivity to voltage.

$b$  : Strength of calcium-gated potassium channels.

$b_1$  : Baseline rate of calcium uptake.

$k$  : Rate of cytosolic calcium decay.

$\phi$  : Timescale for potassium channel dynamics.

$\epsilon$  : Timescale for cytosolic calcium dynamics.

# The Fast System

- Assume that changes in calcium are negligibly small. So  $\epsilon = z' = 0$ .
- The value of  $z$  is now a parameter.

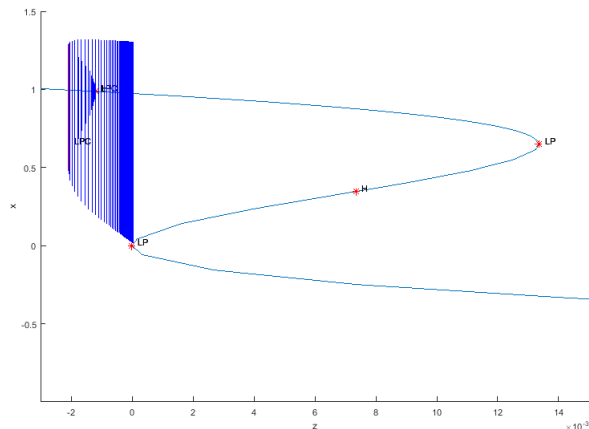
$$\begin{aligned}x' &= -s(-ax^3 + x^2) - y - bz \\y' &= \phi(x^2 - y)\end{aligned}\tag{9}$$

- Studying dynamics here can tell us about the full system
  - Example in full-system bursting: loss of fixed-point stability  $\rightarrow$  beginning of active phase, and loss of limit cycle stability  $\rightarrow$  end of active phase [1].

- Used numerical methods
- Found curves of Hopf, saddle-node of fixed points (SNf), saddle-node of periodic orbits (SNp), and homoclinic bifurcations.
- Codimension-2 bifurcations occur at the intersections of these curves [1]



# Codimension-1 Bifurcation Diagram



Codimension-1 bifurcation diagram for the fast system. Two saddle-nodes of fixed points occur at  $z = 0$  and  $z = 0.01336$  and a saddle-node of periodic orbits exists at  $z = -0.002064$  and  $z = -0.001193188$  where stable and unstable periodic orbits collide. A Hopf bifurcation exists at  $z = -0.001199265$  as well as a neutral saddle.

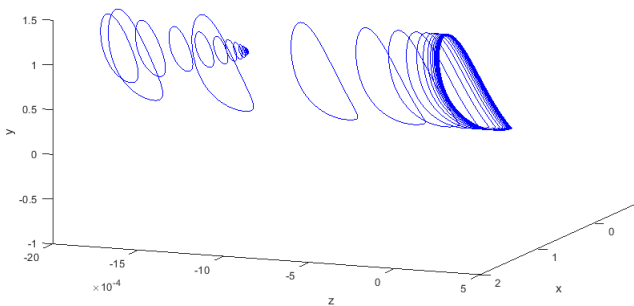


**Figure:** 3-D Extension of bifurcation diagram in previous figure. From Hopf bifurcation at  $z = 0.001199265$ , there are unstable periodic orbits becomes stable periodic orbits and then collide into one homoclinic orbit.

# Numerical Simulation Results

Using XPPaut and MatCont, we have reproduced and expanded the results in [1] have begun to prove the existence of some of these bifurcations as further work.

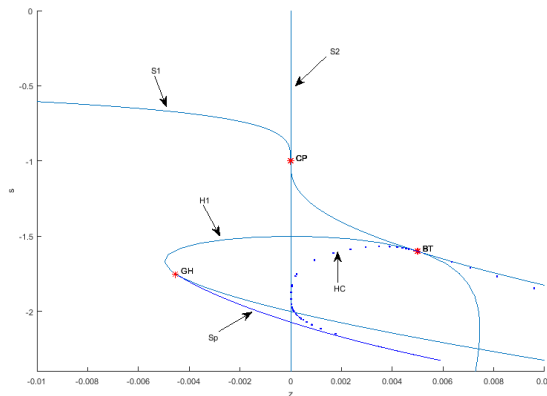
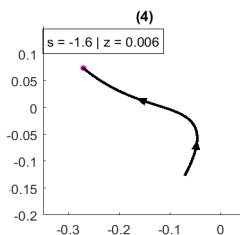
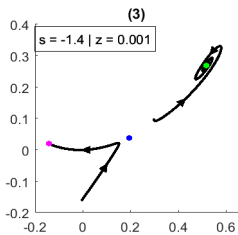
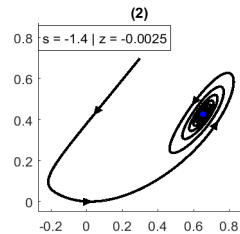
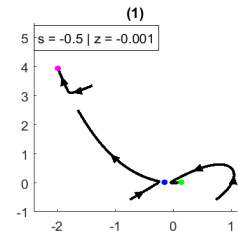
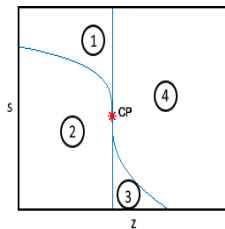
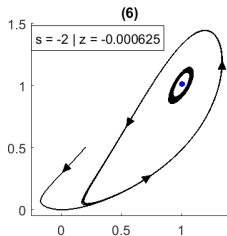
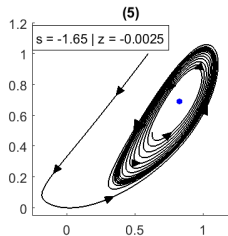
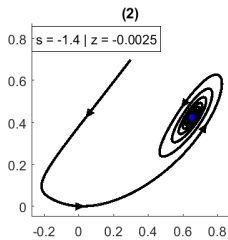
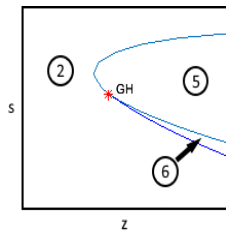


Figure: Codimension-2 bifurcation diagram for the fast system.

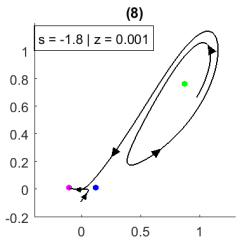
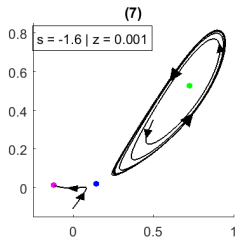
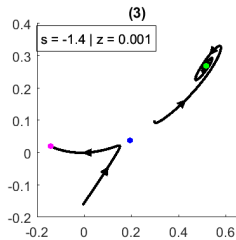
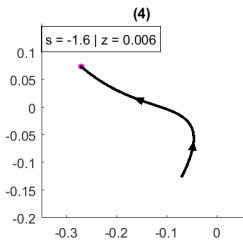
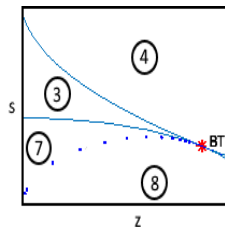
# Cusp



# Generalized Hopf



# Bogdanov-Takens



# Branch of Homoclinic Orbits

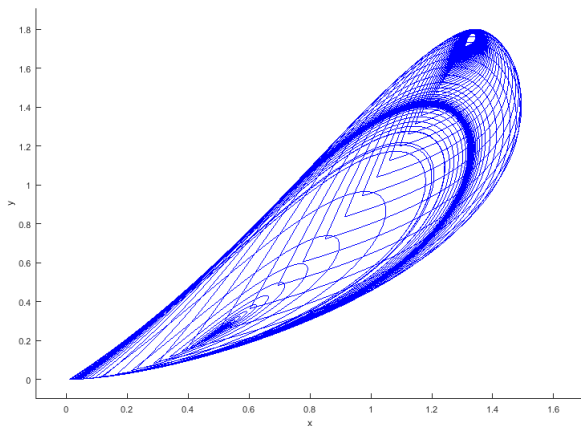


**Figure:** Branch of homoclinic connections out of Bogdanov-Takens point from previous figure.

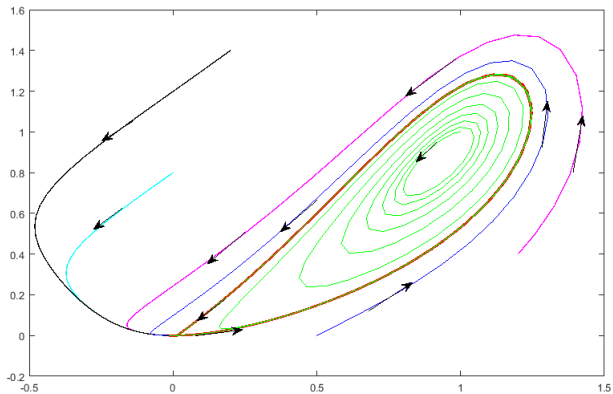


**Figure:** One homoclinic connection grabbed from previous figure in red. Starting from different points around this orbit, different behavior occurs.



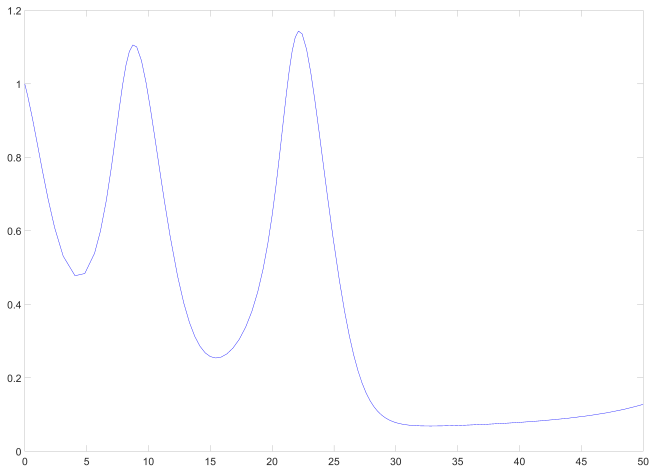


**Figure:** Time series plot of one of the solutions inside of the homoclinic orbit from previous figure.

# Proof for Saddle-node Bifurcation in the Fast System

## Proposition

*The system (9) has a saddle-node bifurcation at the equilibrium point  $(x_0, y_0) = (x^*, x^{*2})$ , where  $x^* > 0$ .*

## Proof.

The Jacobian at this point is

$$J(x_0, y_0) = \begin{bmatrix} 3sax^{*2} - 2sx^* & -1 \\ 2\phi x^* & -\phi \end{bmatrix}$$

The eigenvalues of this matrix satisfy the characteristic polynomial

$$\lambda^2 + \lambda \left( \phi + 2sx^* - 3asx^{*2} \right) - 3a\phi sx^{*2} + 2\phi x^*(1 + s) = 0$$



## Proof.

Sotomayor's Theorem requires one of these eigenvalues to be 0. Therefore, the following condition must be solved:

$$-3asx^{*2} + 2\phi x^*(1 + s) = 0$$

the corresponding bifurcation value of  $z$  is

$$z_0 = -\frac{4}{27} \frac{s^3 + 3s^2 + 3s + 1}{ba^2s^2} \quad (10)$$



Proof.

The right eigenvector of this matrix for  $\lambda = 0$  is

$$v = \begin{bmatrix} 1 \\ 2x^* \end{bmatrix}$$

and the left eigenvector is

$$w^T = [-\phi \quad 1]$$



## Proof.

Finally, check the two conditions:



$$\begin{aligned}w^T f_z(x_0, z_0) &= [-\phi \quad 1] \begin{bmatrix} -b \\ 0 \end{bmatrix} \\ &= \phi b \\ &\neq 0\end{aligned}$$



$$\begin{aligned}w^T D^2 f(x_0, z_0)(v, v) &= [-\phi \quad 1] \begin{bmatrix} 6sax^* - 2s \\ 2\phi \end{bmatrix} \\ &= -\phi(6sax^* - 2s) + 2\phi \\ &\neq 0\end{aligned}$$

Both conditions are satisfied, so a saddle-node bifurcation exists by Sotomayor's Theorem. □

# Proof for Hopf Bifurcation in the Fast system

## Proposition

*Under certain conditions, the system (9) exhibits subcritical and supercritical Hopf bifurcations.*

## Proof.

Shifting the variables such that the equilibrium point is the origin:

$$u = x - x_0$$

$$v = y - y_0$$

and renaming  $u, v$  as  $x, y$  gives the following shifted system:

$$x' = (x + x_0)^2(sa(x + x_0) - s) - (y + y_0) - bz$$

$$y' = \phi(x + x_0)^2 - \phi(y + y_0)$$



Proof.

The expansion of the shifted system gives

$$\begin{aligned}x' = & (-sx_0^2 + asx_0^3 - y_0 - bz) - y + O(|y|^4) + \\ & (2sx_0 + 3asx_0^2)x + \\ & (-s + 3asx_0)x^2 + \\ & asx^3 + O(|x|^4)\end{aligned}$$

$$\begin{aligned}y' = & (\phi x_0^2 - \phi y_0) - \phi y \\ & + O(|y|^4) + 2\phi x_0 x \\ & + \phi x^2 + O(|x|^4)\end{aligned}$$



## Proof.

and the Lyapunov number is

$$\sigma = \frac{3\pi(4\phi x_0(-s + 3asx_0))}{2(\phi x_0(2s - 3asx_0 + 2))^{3/2}}$$

with conditions  $x_0 < \frac{2(1+s)}{3as}$  and  $x_0 \neq \frac{1}{3a}$  we have  $\sigma \neq 0$   
so a Hopf bifurcation occurs.

Under certain conditions for the equilibrium  $(x_0, y_0) = (x^*, x^{*2})$  to be center, the system (9) exhibits subcritical and supercritical Hopf bifurcations.

In the expansion of the shifted system,  $a_{01} = -1$ ,  
 $a_{10} = 2sx_0 + 3asx_0^2$ ,  $a_{20} = -s + 3asx_0$ ,  $a_{30} = as$ , and  $b_{01} = -\phi$ ,  
 $b_{10} = 2\phi x_0$ ,  $b_{20} = \phi$

The Jacobian of system (9) at  $(x^*, x^{*2})$  (or the shift system at  $(0,0)$ ) must have a determinant  $D > 0$  and a trace  $\tau = 0$  for  $(x^*, x^{*2})$  to be center.





## Proof.

The Jacobian at this point is

$$J(x_0, y_0) = \begin{bmatrix} 3sax^{*2} - 2sx^* & -1 \\ 2\phi x^* & -\phi \end{bmatrix}$$

The determinant of this Jacobian is

$$D = -3\phi sax^{*2} + 2\phi x^*(s + 1)$$

and the trace is

$$\tau = 3sax^{*2} - 2sx^* - \phi$$



## Proof.

Combine the conditions of Lyapunov number, we obtain, For  $\sigma < 0$ ,  $x^* < \frac{1}{3a}$ , and for  $\sigma > 0$ ,  $\frac{1}{3a} < x^* < \frac{2(1+s)}{3as}$ . Numerical calculations show that when  $a = 0.5$ ,  $\phi = 1$ ,  $s = -1.6$ , and  $x^* = -1$ , we get  $\sigma = -32.0991$ . For  $a = 0.5$ ,  $\phi = 1$ ,  $s = -2$ , and  $x^* = 1$ , we get  $\sigma = 94.2478$ . Therefore there exists an open set  $S_{11}$  in the parameter space  $(a, \phi, s)$  such that  $\sigma < 0$  and all of our restrictions hold:

$$S_{11} = \{(a, \phi, s) : D > 0, \tau = 0, \text{ and } \sigma_1 < 0\}$$

Similarly, another set  $S_{12}$  exists such that

$$S_{12} = \{(a, \phi, s) : D > 0, \tau = 0, \text{ and } \sigma_1 > 0\}$$

The surface  $H_{p1} = \{(a, \phi, s) : (a, \phi, s) \in S_{11}\}$  is the supercritical Hopf bifurcation of the system (9) and the surface  $H_{b1} = \{(a, \phi, s) : (a, \phi, s) \in S_{12}\}$  is the subcritical Hopf bifurcation of the system (9). □

# Theorem for Local Stability of Fast system

In (9), for  $y' = 0$  we need all equilibrium points to satisfy  $(x_0, y_0) = (x^*, x^{*2})$ , then plug  $y_0 = x^{*2}$  in  $x' = 0$ , we obtain the equation:

$$sax^{*3} - (s + 1)x^{*2} - bz = 0 \quad (11)$$

In the fast system,  $s$ ,  $a$ ,  $b$  are fixed positive parameters and  $z$  is varied. Hence we have  $sa > 0$ ,  $-(s + 1) < 0$  and  $-bz$  could be positive or negative. So the sign of the equation (11) could change once or twice. By Descartes's Rule of signs, then there could be none or one or two equilibrium points which are the positive real roots of the first equation of (9) when we are changing the parameter  $z$ .

Compute:

$$\tau^2 - 4D = (3sax^{*2} - 2sx^* - \phi)^2 - 4(-3\phi sax^{*2} + 8\phi x^*(s + 1))$$

with

$$-4D = 4\phi^2 - 8\phi x^* + 4\phi(3sax^{*2} - 2sx^* - \phi)$$

$$\tau = 3sax^{*2} - 2sx^* - \phi$$

Therefore

$$\begin{aligned}\tau^2 - 4D &= \tau^2 + 4\phi\tau + 4\phi^2 - 8\phi x^* \\ &= (\tau + 2\phi)^2 - 8\phi x^*\end{aligned}$$

$$\tau^2 - 4D \geq 0 \iff$$

$$(\tau + 2\phi)^2 - 8\phi x^* \geq 0 \tag{12}$$

$$8\phi x^* \leq (\tau + 2\phi)^2$$

$$x^* \leq \frac{(\tau + 2\phi)^2}{8\phi}$$

We solve

$$\tau = 0 \iff 3sax^{*2} - 2sx^* - \phi = 0$$

(13)

with  $x^* > 0$  and  $\phi \leq \frac{5}{3a}$ , we obtain:

$$x^* = \frac{2s + \sqrt{4s^2 - 12sa\phi}}{6sa}$$

The vertex of the parabola (13) is  $(\frac{1}{3a}, \frac{-s}{3a})$

With the condition  $x^* > 0$ , we will only look at the range

$$0 < x^* < \frac{2s + \sqrt{4s^2 - 12sa\phi}}{6sa} \text{ and } x^* > \frac{2s + \sqrt{4s^2 - 12sa\phi}}{6sa}.$$

Thus, we have established the following result:

## Theorem

The equilibrium point has the following local stability properties:  
Since  $x^* < \frac{2(1+s)}{3sa}$  based on the condition of Lyapunov number in proposition 2,

- 1 (9) has no saddle at  $(x^*, x^{*2})$ .
- 2 if  $x^* \leq \frac{(T+2\phi)^2}{8\phi}$ , then (9) has a node at  $(x^*, x^{*2})$ ;
  - it is stable if  $x^* < \frac{2s + \sqrt{4s^2 - 12sa\phi}}{6sa}$  causing  $\tau < 0$ .
  - it is unstable if  $x^* > \frac{2s + \sqrt{4s^2 - 12sa\phi}}{6sa}$  causing  $\tau > 0$ .
- 3 if  $x^* > \frac{(T+2\phi)^2}{8\phi}$ , and  $\tau \neq 0$  then (9) has a focus at  $(x^*, x^{*2})$ ;
  - it is stable if  $x^* < \frac{2s + \sqrt{4s^2 - 12sa\phi}}{6sa}$  causing  $\tau < 0$ .
  - it is unstable if  $x^* > \frac{2s + \sqrt{4s^2 - 12sa\phi}}{6sa}$  causing  $\tau > 0$ .

## Theorem

Suppose that the following assumptions are satisfied:

- 1 There exists function  $D_i : U \rightarrow R$ ,  $G_{ij} : U \rightarrow R$  and constant  $a_{ij} \geq 0$  such that for every  $1 \leq i \leq n$ ,  
 $D'_i = D'_i|_{(3.6)} \leq \sum_{j=1}^n a_{ij} G_{ij}(z)$  for  $z \in U$ .
- 2 For  $A = [a_{ij}]$ , each directed cycle  $C$  of  $(G, A)$  has  
 $\sum_{(s,r) \in (C)} G_{rz}(z) \leq 0$  for  $z \in U$ , where  $(C)$  denotes the arc set of the directed cycle  $C$ .

Then, the function

$$D(z) = \sum_{i=1}^n c_i D_i(z) \quad (14)$$

with constant  $c_i \geq 0$  satisfies  $D' = D'|_{(3.6)} \leq 0$ ; that is,  $D$  is a Lyapunov function [5].



# Construction of Lyapunov Function to Prove Global Stability of the Fast System

## Proposition

*There exists a Lyapunov function for the equilibrium point  $(x^*, x^{*2})$  if  $x$  and  $y$  satisfy the conditions  $0 < x < \frac{x^*}{e}$  and  $0 < y < y^*$ .*

## Proof.

We have at the equilibrium point  $(x^*, y^*)$  with  $y^* = x^{*2}$ , so substituting this into the first equation in (9), we obtain

$$bz = sax^{*3} - sx^{*2} - y^*.$$


## Proof.

Construction: Let  $D_1 = x - x^* - x^* \ln \frac{x}{x^*}$  and  $D_2 = y - y^* - y^* \ln \frac{y}{y^*}$ . We will also use the inequality  $1 - x + \ln x \leq 0$  for  $x > 0$  with equality holding if and only if  $x = 1$ . Differentiation gives

$$\begin{aligned} D_1' &= \frac{x - x^*}{x} x' \\ &= \frac{x - x^*}{x} (sax^3 - sx^2 - y - (bz)) \\ &= \frac{x - x^*}{x} (sax^3 - sx^2 - y - (sax^{*3} - sx^{*2} - y^*)) \\ &= \left(1 - \frac{x^*}{x}\right) (sa(x^3 - x^{*3}) - s(x^2 - x^{*2}) - (y - y^*)) \end{aligned}$$



## Proof.

since  $0 < x < x^*$  and  $0 < y < y^*$  we have

$sa(x^3 - x^{*3}) < 0$ ,  $-s(x^2 - x^{*2}) > 0$ ,  $\ln \frac{x}{x^*} < 0$ ,  $(y - y^*) < 0$  and

$$\left(1 - \frac{x^*}{x}\right) \leq \ln \frac{x}{x^*}$$

so  $D'_1 \leq \ln \frac{x}{x^*} (-s(x^2 - x^{*2}) - (y - y^*)) =: a_{12} G_{12}$

and similarly

$$\begin{aligned} D'_2 &= \frac{y - y^*}{y} y' \\ &= \frac{y - y^*}{y} \phi(x^2 - y) \\ &= \phi\left(x^2 \left(1 - \frac{y^*}{y}\right) - (y - y^*)\right) \\ &\leq \phi\left(x^2 \ln \frac{y}{y^*} - (y - y^*)\right) =: a_{21} G_{21} \end{aligned}$$



Proof.

with  $a_{12} = 1 > 0$ ,  $a_{21} = \phi > 0$  and

$$G_{12} = \ln \frac{x}{x^*} (-s(x^2 - x^{*2}) - (y - y^*)), \quad G_{21} = x^2 \ln \frac{y}{y^*} - (y - y^*)$$

We have

$$\begin{aligned} G_{12} + G_{21} &= \ln \frac{x}{x^*} (-s(x^2 - x^{*2}) - (y - y^*)) + x^2 \ln \frac{y}{y^*} - (y - y^*) \\ &= -s \ln \frac{x}{x^*} (x^2 - x^{*2}) + x^2 \ln \frac{y}{y^*} - (y - y^*) \left( \ln \frac{x}{x^*} + 1 \right) < 0 \end{aligned}$$

with the initial conditions of  $x$  and  $y$ .



## Proof.

So by Theorem 7, there exists  $c_1$  and  $c_2$  such that  $D = c_1 D_1 + c_2 D_2$  is a Lyapunov function for (9). Since  $d^+(2) = 1$ , Theorem 9 implies that  $c_1 = \phi c_2$ . Therefore, a Lyapunov function  $D = \phi D_1 + D_2$  can be used to prove the global stability of the equilibrium point  $(x^*, x^{*2})$ .

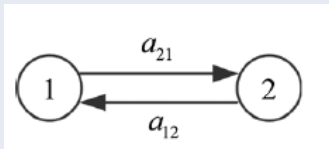


Figure: Digraph constructed for the fast system (9)



The full model of the Hindmarsh-Rose system is:

$$\begin{aligned}x' &= sax^3 - sx^2 - y - bz \\y' &= \phi(x^2 - y) \\z' &= \varepsilon(sa_1x + b_1 - kz)\end{aligned}\tag{15}$$

The key ingredient that we found in the fast system is the existence of a saddle-node of periodic orbits which indicates the existence of torus canards in the full system. The torus bifurcation is between the transition from spiking to bursting in neurons where the stable periodic orbits indicate rapid spiking in the neuron and the unstable periodic orbits indicate rapid bursting.

# Codimension-1 Bifurcation Diagram

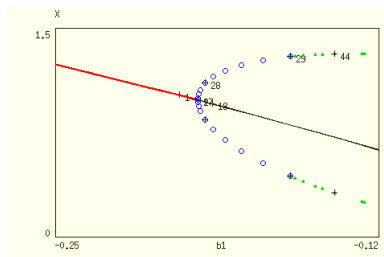


**Figure:** Codimension-1 bifurcation diagram for the full system. The red/black curve represents a branch of fixed points going from stable to unstable with a curve of periodic orbits forming at the Hopf bifurcation at  $b_1 = -0.1927$ . These periodic orbits go from unstable to stable with Torus bifurcations occurring where the periodic orbits go from stable to unstable and unstable to stable at  $b_1 = -0.1926$  and  $b_1 = -0.1603$  respectively.

# Torus Bifurcation in the Full System

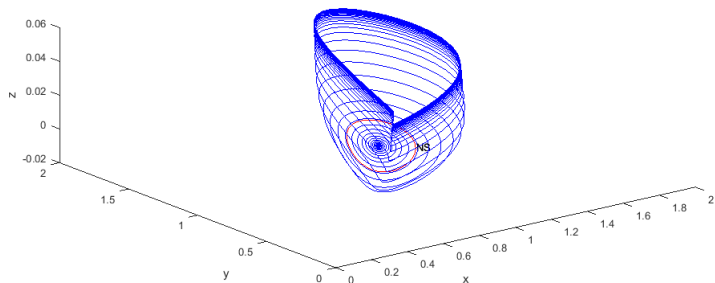
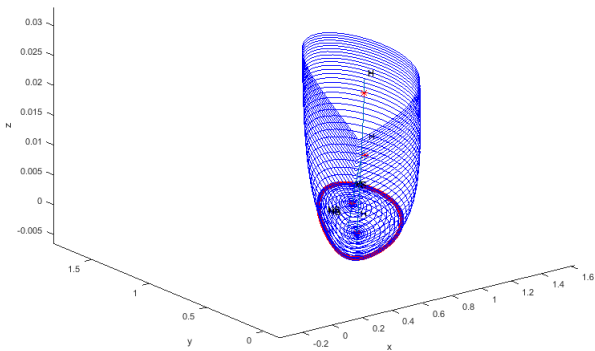


**Figure:** Torus bifurcation diagram for the full system occurs at  $b_1 = -0.19267225$ . The red cycle *NS* is where torus bifurcation occurs that stable periodic orbits inside *NS* curve become unstable and go into the blue unstable surface.





Az: 17 E: -13

**Figure:** Extension of previous figures in the  $xyz$  space. We obtained three more Hopf bifurcations and two more Torus bifurcations which occur at  $b_1 = -0.1602552$ , and  $b_1 = -0.16046985$ .

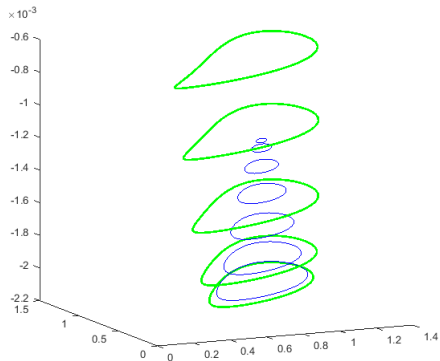
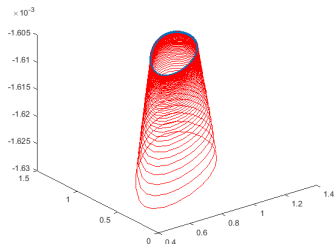
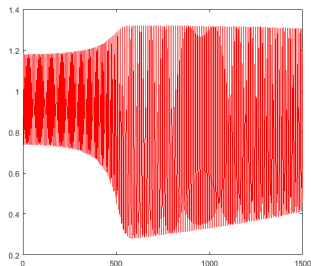


**Figure:** Stable (green) and unstable (blue) periodic orbits seen in previous figure that collide together at a Torus bifurcation.



Unstable periodic orbit in blue. Starting from a point near the unstable orbit, the solution (red) spirals away into a Torus.



Time series plot.

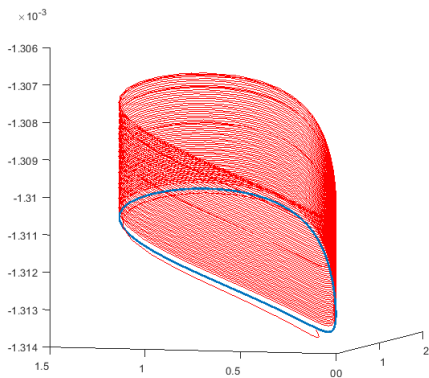


**Figure:** Stable periodic orbit in blue. Starting from a point near the stable orbit, the solution (red) at first spirals out but then spirals back into the orbit.

# Torus Canard

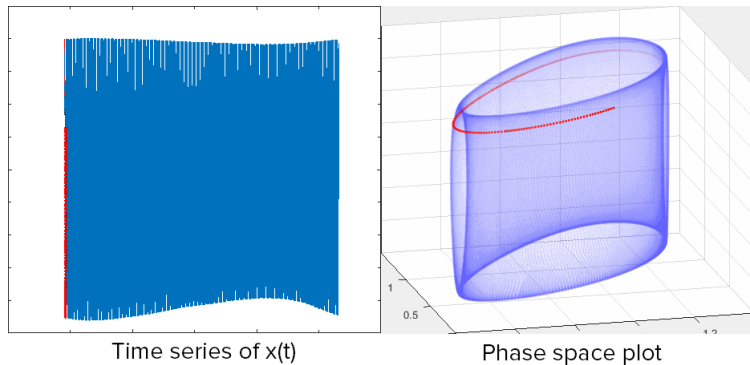


**Figure:** An animation displaying torus canard behavior in (15).

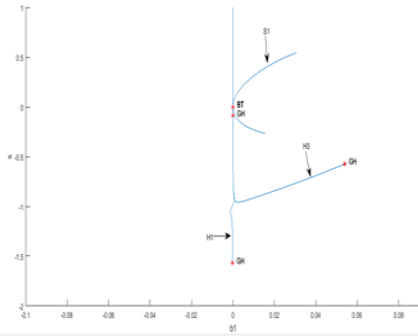
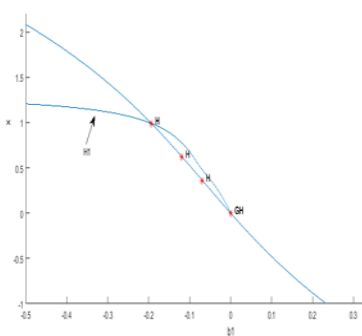


Figure: Generalized Hopf and Bogdanov-Takens bifurcation diagrams

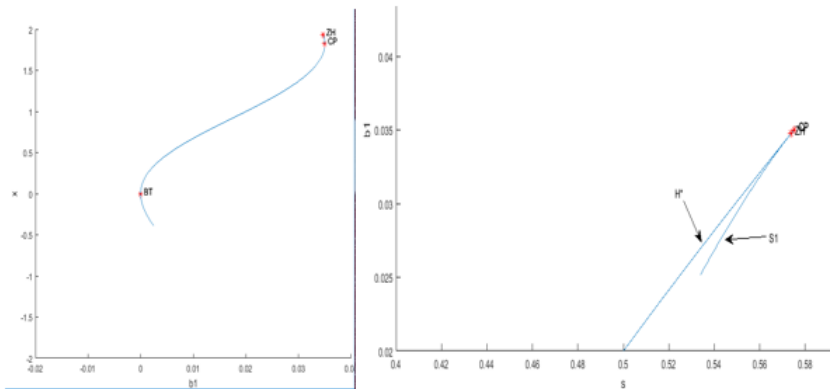
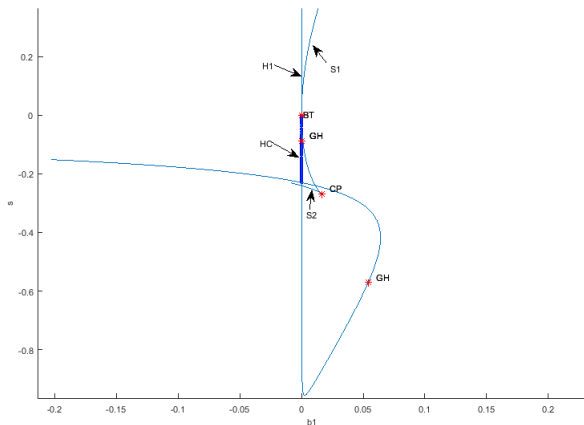


Figure: Cusp and Zero-Hopf bifurcation



Homoclinic curve out of Bogdanov-Takens bifurcation from previous figure in solid blue. One Hopf bifurcation curve labeled H1, two saddle-node curves labeled S1, S2, two GH-generalized Hopf bifurcations at  $(b_1, s) \approx (0, -0.088622)$  and  $(0.05399, -0.57108)$ , and a cusp bifurcation at  $(0.01628, -0.26748)$ . The Hopf bifurcation curve goes right through the homoclinic curve.



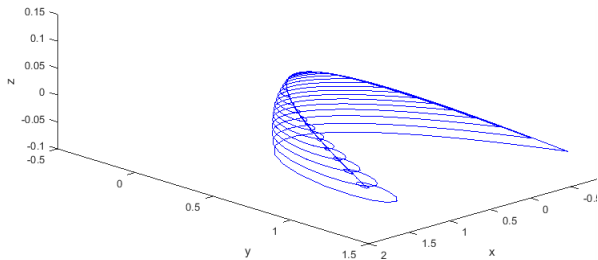


















Figure: Solution curves from homoclinic connection in Figure 87.

- Computed more codimension-1 and codimension-2 bifurcations for fast and full systems.
- Extended bifurcation regions and bifurcation boundaries, helping explain more complex dynamics.
- Provided proofs for the existence of some of the codimension-1 bifurcations.

- Provide a detailed description of the dynamics of the H-R model by completing and extending our current bifurcation analysis.
- Provide existence proofs for some codimension-2 bifurcations.
- Obtain global stability results with larger (less restrictive) attracting sets via graph-theoretic methods.
- Completing the proof for global stability of the fast system by applying LaSalle's Principle.
- Discover other bifurcations in the system. Possibility of heteroclinic orbits?

-  J. Burke, M. Desroches, A. Barry, T. Kaper, M. Kramer, *A showcase of torus canards in neuronal bursters*, J. of Mathematical Neuroscience **2** (2012), DOI: 10.1186/2190-8567-2-3.
-  Nathalie Corson, Moulay Aziz-Alaoui. Asymptotic dynamics of Hindmarsh-Rose neuronal system. Dynamics of Continuous, Discrete and Impulsive Systemes, Series B: Applications and Algorithms, 2009, p.535. jhal-00952598;
-  D. DeBolt. *Application of the Hindmarsh-Rose Neuronal Model in Electronic Circuits*. Northeastern University Department of Electrical and Computer Engineering. May 2011. Web. 25 July 2017.
-  A. Dhooge, W. Govaerts, Y. Kuznetsov, *MATCONT: A MATLAB package for numerical bifurcation analysis of ODEs*, ACM Transact. on Math. Softw. **29** (2003), 141–164.
-  E. Doedel, A. Champneys, T. Fairgrieve, R. Paffenroth, Y. Kuznetsov, B. Sandstede, X.J. Wang, AUTO 2000: *Continuation and bifurcation software for ordinary differential*

-  I. Eugene. *Neural Excitability, Spiking and Bursting*. International Journal of Bifurcation and Chaos. **6** (2000): 1171-1266.
-  M. Gatto, L. Mari, E. Bertuzzo, R. Casagrandi, L. Righetto, I. Rodriguez-Iturbe, A. Rinaldo, *Generalized reproduction numbers and the prediction of patterns in waterborne disease*, Proceed. Nat. Acad. of Scienc. **109** (2012), 1-6.
-  J. Guckenheimer, Y. Kuznetsov. "Bautin bifurcation." Scholarpedia. N.p., n.d. Web. 25 July 2017.
-  J. Guckenheimer, Y. Kuznetsov. "Bogdanov-Takens Bifurcation." Scholarpedia. N.p., n.d. Web. 25 July 2017.
-  K. Tsaneva-Atanasova, H.M. Osinga, T. Rieß, A. Sherman. *Full System Bifurcation Analysis of Endocrine Bursting Models*. *Journal of Theoretical Biology*. 21 June 2010. Web. 20 June 2017.

-  Y. Kuznetsov. *Elements of applied bifurcation theory*. 2nd ed. New York: Springer, 1998.
-  M. Mohameed Follow. "7 neurons." LinkedIn SlideShare. N.p., 01 Dec. 2010. Web. 25 July 2017.
-  L. Perko. *Differential equations and dynamical systems*. 3rd ed. New York: Springer, 2001.
-  J. Rebaza. *A First Course in Applied Mathematics*. Wiley 2012.
-  Z. Shuai, P. Van Den Driessche, *Global stability of infectious disease models using Lyapunov functions*, SIAM J. Appl. Math. **73** (2013): 1513-1532.
-  B. Ermentrout. *Simulating, Analyzing, and Animating Dynamical Systems*, SIAM (2002).